

PROCEEDINGS OF SPIE

SPIDigitalLibrary.org/conference-proceedings-of-spie

Isotropic-resolution linear-array-based photoacoustic computed tomography through inverse Radon transform

Guo Li, Jun Xia, Lei Li, Lidai Wang, Lihong V. Wang

Guo Li, Jun Xia, Lei Li, Lidai Wang, Lihong V. Wang, "Isotropic-resolution linear-array-based photoacoustic computed tomography through inverse Radon transform," Proc. SPIE 9323, Photons Plus Ultrasound: Imaging and Sensing 2015, 93230I (11 March 2015); doi: 10.1117/12.2076660

SPIE.

Event: SPIE BiOS, 2015, San Francisco, California, United States

Isotropic-resolution linear-array-based photoacoustic computed tomography through inverse Radon transform

Guo Li, Jun Xia, Lei Li, Lidai Wang and Lihong V. Wang*

Optical Imaging Laboratory, Department of Biomedical Engineering, Washington University in St. Louis, One Brookings Drive, St. Louis, Missouri 63130

*Corresponding author: lhwang@biomed.wustl.edu

ABSTRACT

Linear transducer arrays are readily available for ultrasonic detection in photoacoustic computed tomography. They offer low cost, hand-held convenience, and conventional ultrasonic imaging. However, the elevational resolution of linear transducer arrays, which is usually determined by the weak focus of the cylindrical acoustic lens, is about one order of magnitude worse than the in-plane axial and lateral spatial resolutions. Therefore, conventional linear scanning along the elevational direction cannot provide high-quality three-dimensional photoacoustic images due to the anisotropic spatial resolutions. Here we propose an innovative method to achieve isotropic resolutions for three-dimensional photoacoustic images through combined linear and rotational scanning. In each scan step, we first elevationally scan the linear transducer array, and then rotate the linear transducer array along its center in small steps, and scan again until 180 degrees have been covered. To reconstruct isotropic three-dimensional images from the multiple-directional scanning dataset, we use the standard inverse Radon transform originating from X-ray CT. We acquired a three-dimensional microsphere phantom image through the inverse Radon transform method and compared it with a single-elevational-scan three-dimensional image. The comparison shows that our method improves the elevational resolution by up to one order of magnitude, approaching the in-plane lateral-direction resolution. *In vivo* rat images were also acquired.

Keywords: photoacoustic computed tomography; linear transducer array; inverse Radon transform; isotropic resolution

1. INTRODUCTION

Photoacoustic computed tomography (PACT) is an emerging imaging modality that ultrasonically breaks through the optical diffusion limit by combining both optical contrasts and ultrasonic spatial resolutions.¹ To accelerate imaging speed, PACT usually uses many transducer elements configured at different positions to detect photoacoustic waves, and then reconstructs an image using advanced algorithms. Although curved transducer arrays, such as ring-shape arrays^{2,3} and spherical arrays⁴, can obtain high-quality PACT images, they are usually customized and expensive. Moreover, they need accessibility from multiple sides of the target. In comparison, one-dimensional (1D) linear transducer arrays can form images from just one side of the sample. They are readily available at low cost, and offer hand-held convenience. However, conventional three-dimensional (3D) images acquired by linear-array PACT through linear scans along the transducer's elevational direction have low image quality due to anisotropic spatial resolutions. Here, we define the axial resolution as the spatial resolution along the acoustic axis, the lateral resolution as the spatial resolution along the row of elements of the array, and the elevational resolution as the spatial resolution along the direction normal to the B-scan image plane of the linear transducer array. The axial resolution is limited by both the speed of sound of the acoustic medium and the bandwidth of the transducer elements. The lateral resolution is mainly determined by the axial resolution and the synthetic aperture of the transducer array relative to the image reconstruction region. Usually the lateral resolution is a little worse than the axial resolution. However, the elevational resolution, which is determined by the element length and the cylindrical acoustic lens focus, is usually one order of magnitude worse than the axial resolution. Thus the poor elevational resolution will blur features along the elevational direction, and consequently yield conventionally stacked 3D images of low quality.

To improve the 3D image quality with a linear transducer array, a two-dimensional (2D) array probe might be used.⁵ But a 2D array costs much more than a 1D linear array. Song et al. proposed a section-illumination setup and improved the elevational resolution by 10 times over that of a single direction scan without section illumination.⁶ But section-illumination still depends on the optical focusing effect, and the elevational resolution degrades quickly to the acoustically defined elevational resolution beyond one transport mean free path. Jerome et al. explored using a combined linear and rotation scan to achieve nearly isotropic 3D spatial resolution.⁷⁻⁹ However, their configurations enclosed the object and required access around the object in a cylindrical pattern, which works only for imaging small animals. Recently, Schwarz et al.¹⁰ proposed a bi-directional scan method to improve the spatial resolution, but the resulting spatial resolution was not uniform in all directions, and taking the geometric mean lacks physical meaning. Here we propose a new method of elevationally scanning a linear transducer array in multiple directions and reconstructing 3D images by using the inverse Radon transform (IRT), which is a standard image reconstruction method in X-ray CT. We call this method IRT-PACT.

2. EXPERIMENTAL SETUP

The IRT-PACT setup is shown schematically in Fig. 1. A commercial linear transducer array with 256 elements (LZ250, 21 MHz central frequency, 11 MHz bandwidth, Visualsonics Inc., Canada) is the photoacoustic wave detector. The LZ250 array integrates an optical fiber bundle with a dark-field illumination pattern at the end of the probe. The focal length of the cylindrical acoustic lens is 15 mm. More details about the LZ250 array can be found in Ref. [11]. A 20 Hz laser with 532 nm wavelength is coupled into the fiber bundle of the probe. The output laser pulse has an average intensity of $\sim 8 \text{ mJ/cm}^2$ on the target tissue's surface, within the ANSI safety limit (20 mJ/cm^2). To homogenize the incident laser light and acoustically couple the PA waves, a layer of a mixture of ultrasonic gel and 1% intralipid solution is applied on the target tissue's surface, which is in contact with a flexible polyethylene membrane window in the bottom of a water-filled tank. The LZ250 array is submerged in the water-filled Petri dish for acoustic coupling. A commercial photoacoustic imaging platform (Vevo LAZR, Visualsonics Inc., Canada) is used to acquire photoacoustic images. Due to the four-to-one multiplexer in the image acquisition system, the B-scan frame rate is 5 frames/sec at a laser repetition rate of 20 Hz.

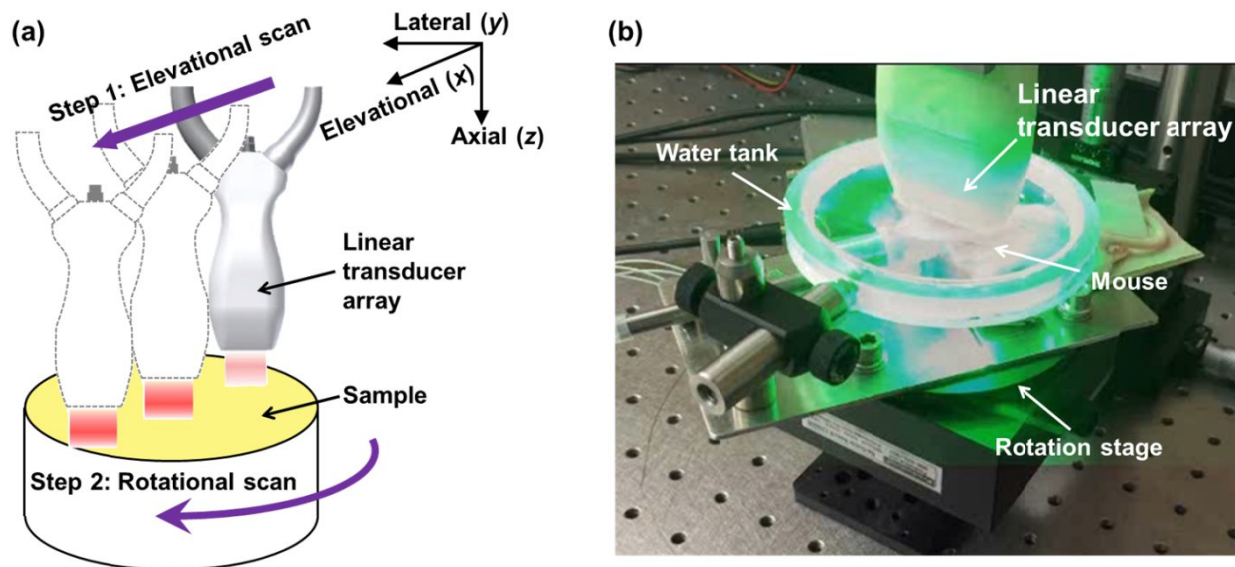


Fig. 1. (a) Schematic of the scanning setup of the IRT-PACT; (b) Photo of the experimental setup.

In IRT-PACT, the sample is rotated in increments and linearly scanned at each angular position, as shown in Fig. 1(a). For comparison, we call PACT with a single linear scan along the elevational direction of the transducer array at the first rotational angle “conventional PACT”. Rotational scanning was realized by a motorized rotation stage (Productrial LLC,

USA). In our study each full data set contains 90 rotations with a 2° angular step size. At each rotation angle, a linear scan along the elevational direction (x) of the linear transducer array was performed by a motorized linear translation stage. The linear scan speed was 2 mm/sec, so each B-scan slice corresponded to 0.4 mm thickness in the elevational direction. The linear scan range at each rotation angle was 20 mm, corresponding to 50 B-scan frames. Thus each full data set contained $90 \times 50 = 4500$ B-scan frames, and the total scan time was ~ 16 min (90 linear scans at 10 seconds for each scan, plus 90 two-degree rotation steps at 0.5 second per step), and can be further improved by using a laser with higher repetition rate.

To reconstruct 3D photoacoustic images from the multiple-angle data sets, we first reconstructed all B-scan frames from the RF data received by the transducer elements, using the filtered back-projection algorithm.¹² We then integrated B-scan frames acquired at each rotational angle through a Radon transform process, rendering 90 2D projection images. After that, the inverse Radon transform was applied to the 90 2D projections to get a 3D image. Due to the band-pass frequency response of the transducer elements, the reconstructed B-scan frames present bipolar (i.e., both positive and negative) pixel values. To better represent the real optical absorption, which is always non-negative, we applied the Hilbert transform along the depth direction (z) and then took the absolute value to recover the envelope. Because the direction of the Hilbert transform is orthogonal to those of Radon transform and inverse Radon transform, the envelope extraction will not affect the linearity of the Radon transform and inverse Radon transform.

3. RESULTS

IRT-PACT was first demonstrated by imaging an agar gel phantom which contained a dehydrated leaf skeleton. Figs. 2(a) and 2(b) are maximum amplitude projections (MAPs) along the depths (z) of 3D images acquired by conventional PACT and IRT-PACT. Not only are the line features of the IRT-PACT image sharper than those of the conventional PACT image, but also the spatial resolution along the elevational direction is greatly improved after the inverse Radon transform.

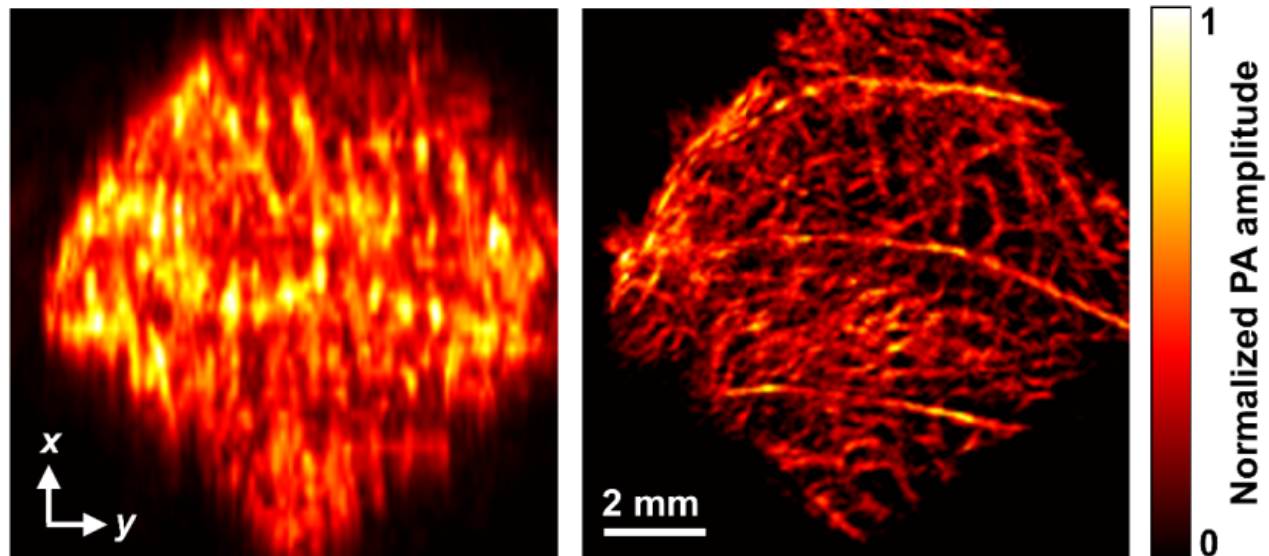


Fig. 2. Leaf phantom images acquired by conventional PACT and IRT-PACT. Maximum amplitude projections along the depths of the conventional PACT image (a) and IRT-PACT image (b).

We also imaged an agar gel phantom which contained two crossed $6 \mu\text{m}$ diameter carbon fibers. Figs. 3(a) and 3(b) are the maximum amplitude projections (MAPs) along the depths (z) of the 3D images acquired by conventional PACT and IRT-PACT. The IRT-PACT image shows features more clearly because of the improved spatial resolutions. Due to the sparse angular sampling, radial artifacts appear in Fig. 3(b), and they can be alleviated by using denser angular sampling, such as a 1° angular step size.

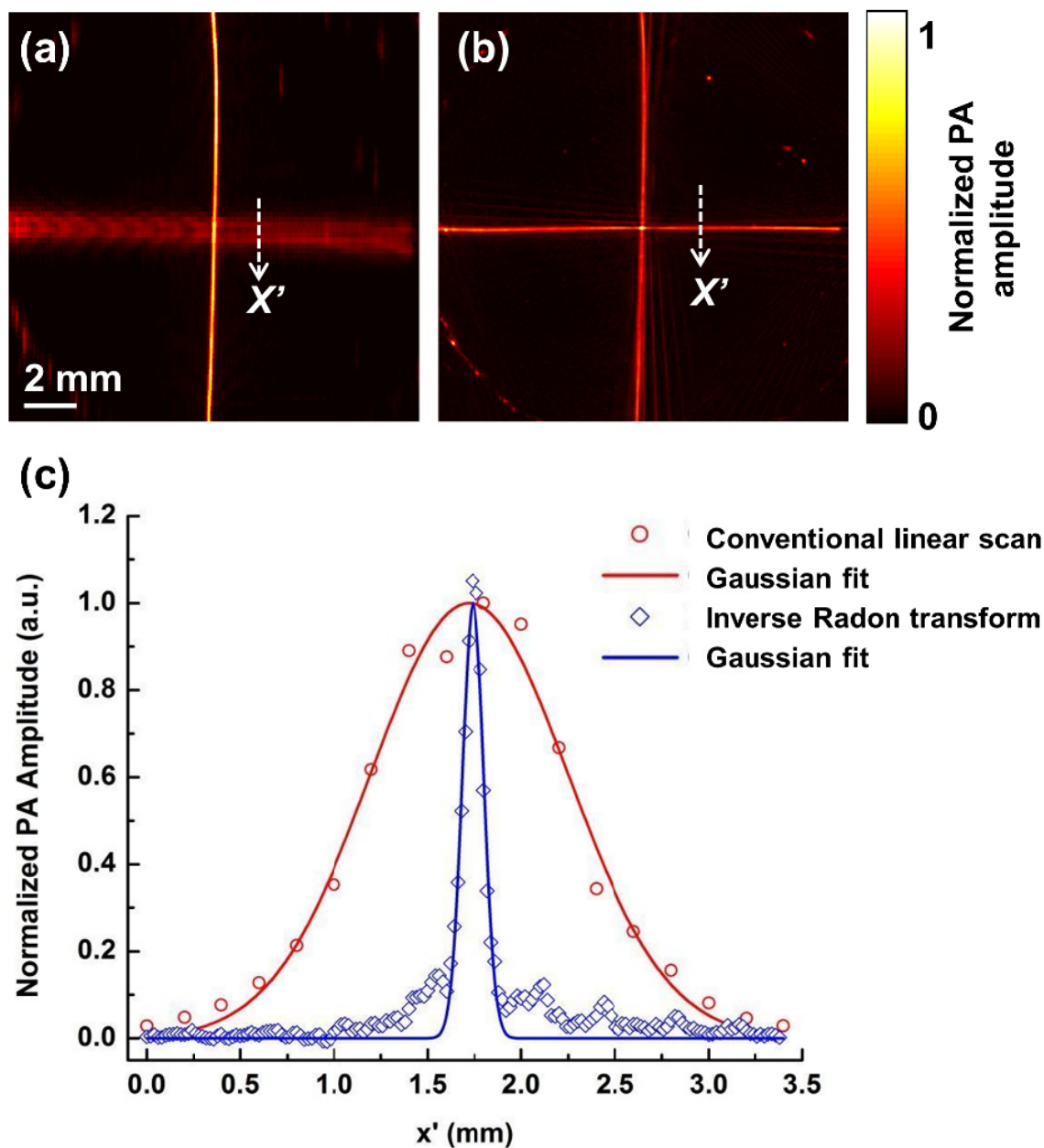


Fig. 3. MAPs of two crossed carbon fibers: (a) conventional linear scan along x' direction; (b) IRT-PACT. (c) Elevational resolution of both conventional PACT and IRT-PACT.

To quantitatively study the elevational resolution improvement, we studied the elevational resolutions of conventional PACT and IRT-PACT, as shown in Fig. 3(c). The elevational resolution of conventional PACT, quantified by fitting the horizontal carbon fiber's profile to a Gaussian pattern along the x' direction, is 1237 μm . The elevational resolution of IRT-PACT by Gaussian fitting the horizontal carbon fiber's profile along the x direction, is 140 μm . Thus the elevational resolution is almost 10 times better.

The improved isotropic resolution can greatly improve the 3D image quality. With single-side access convenience, IRT-PACT can image the rat brain *in vivo* from the top. Here we imaged the brain of a 30-day-old rat (Hsd: Sprague Dawley® SD®, Harlan, Harlan Laboratories Inc., USA) *in vivo* with the scalp intact. The hair was removed before the

imaging experiment. Figs. 4(a) and 4(b) are MAPs of 3D images by conventional PACT and IRT-PACT. Obviously the IRT-PACT images show features more clearly due to the improved spatial resolutions.

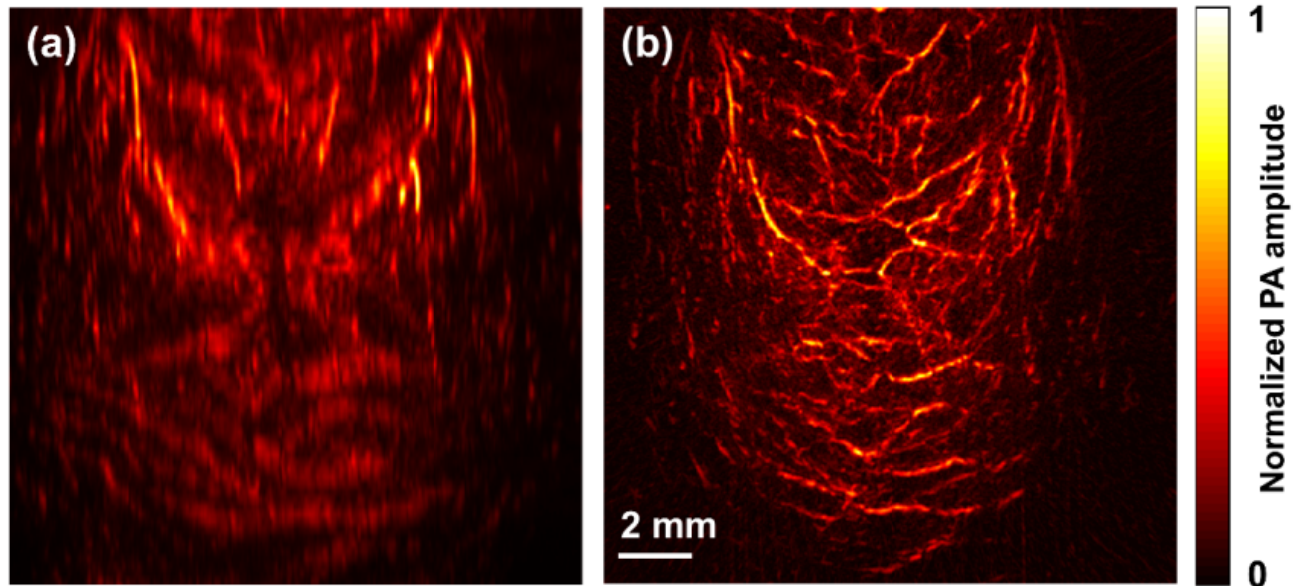


Fig. 4. *In vivo* rat brain images acquired by conventional PACT and IRT-PACT. Maximum amplitude projections along the depths of the conventional PACT image (a) and IRT-PACT image (b).

4. CONCLUSIONS

In summary, we have developed an IRT-PACT system which achieves isotropic resolutions and greatly improves 3D imaging quality. The maximum elevational resolution improvement over conventional PACT is 9.4 times at an imaging depth of 8.3 mm, and can be even larger at smaller imaging depths. *In vivo* mouse brain images have been successfully acquired using the IRT-PACT system. This technology can be applied on all linear-array PACT imaging systems with poor elevational resolution.

5. ACKNOWLEDGMENTS

This work was sponsored by National Institute of Health (NIH) grants DP1 EB016986 (NIH Director's Pioneer Award), R01 CA186567 (NIH Director's Transformative Research Award), U01 NS090579, R01 EB016963, R01 EB010049 and S10 RR026922. L.W. has a financial interest in Microphotoacoustics, Inc. and Endra, Inc., which, however, did not support this work.

REFERENCES

- [1] L. V. Wang and S. Hu, "Photoacoustic Tomography: In Vivo imaging from Organelles to Organs," *Science* 335(6075), 1458-1462 (2012)
- [2] J. Xia, Z. Guo, K. Maslov, A. Aguirre, Q. Zhu, C. Percival and L. V. Wang, "Three-dimensional photoacoustic tomography based on the focal-line concept," *J. Biomed. Opt.* 16(9), 090505 (2011)
- [3] J. Xia, M. R. Chatni, K. Maslov, Z. Guo, K. Wang, M. Anastasio and L. V. Wang, "Whole-body ring-shaped confocal photoacoustic computed tomography of small animals in vivo," *J. Biomed. Opt.* 17(5), 050506 (2012)
- [4] R. A. Kruger, C. M. Kuzmiak, R. B. Lam, D. R. Reinecke, S. P. Del Rio and D. Steed, "Dedicated 3D photoacoustic breast imaging," *Medical Physics* 40(11), 113301 (2013)

- [5] Y. Wang, T. N. Erpelding, L. Jankovic, Z. Guo, J.-L. Robert, G. David and L. V. Wang, "In vivo three-dimensional photoacoustic imaging based on a clinical matrix array ultrasound probe," *J. Biomed. Opt.* 17(6), 061208 (2012)
- [6] L. Song, K. Maslov and L. V. Wang, "Section-illumination photoacoustic microscopy for dynamic 3D imaging of microcirculation in vivo," *Opt. Lett.* 35(9), 1482-1484 (2010)
- [7] J. Gateau, M. A. A. Caballero, A. Dima and V. Ntziachristos, "Three-dimensional optoacoustic tomography using a conventional ultrasound linear detector array: Whole-body tomographic system for small animals," *Medical Physics* 40(1), 013302-013311 (2013)
- [8] J. Gateau, A. Chekkoury and V. Ntziachristos, "High-resolution optoacoustic mesoscopy with a 24 MHz multidetector translate-rotate scanner," *J. Biomed. Opt.* 18(10), 106005 (2013)
- [9] J. Gateau, A. Chekkoury and V. Ntziachristos, "Ultra-wideband three-dimensional optoacoustic tomography," *Optics Letters* 38(22), 4671-4674 (2013)
- [10] M. Schwarz, A. Buehler and V. Ntziachristos, "Isotropic high resolution optoacoustic imaging with linear detector arrays in bi-directional scanning," *Journal of Biophotonics* 8(1-2), 60-70 (2014)
- [11] A. Needles, A. Heinmiller, J. Sun, C. Theodoropoulos, D. Bates, D. Hirson, M. Yin and F. S. Foster, "Development and initial application of a fully integrated photoacoustic micro-ultrasound system," *IEEE Transactions on Ultrasonics, Ferroelectrics and Frequency Control* 60(5), 888-897 (2013)
- [12] M. Xu and L. V. Wang, "Universal back-projection algorithm for photoacoustic computed tomography," *Physical Review E* 71(1), 016706 (2005)